Materials Research. 2020; 23(5): e20200188
DOI: https://doi.org/10.1590/1980-5373-MR-2020-0188

A Molecular Dynamics Study on Polycaprolactone -Metal Oxide Interactions

Nosrat Madadi Mahani*[a]

[a]*Payame Noor University, Department of Chemistry, 19395-4697, Tehran, Iran*

Received: May 03, 2020; Revised: July 25, 2020; Accepted: September 26, 2020

In order to realize the macroscopic features of a number of chemically bonded multi-layer dielectric and composite materials, interactions of metal oxide surfaces, polymer surface atoms, and near-surface atoms are very beneficial. The simulation study of polymer-metal oxides interfaces is of great importance in investigating the adhesion and miscibility features of these systems that are inherently challenging to obtain experimentally or for which there is no experimental data, even if some low data exist, they are not reliable. Polycaprolactone (PCL) is biocompatible, biodegradable, non-toxic and hydrophobic polyester that has been used in tissue engineering, such as a bioactive implant. Hence, the molecular dynamics simulations of PCL are carried out to investigate its surface interaction with metal oxides as ZnO, CuO, Fe_2O_3, NiO and SiO_2. The force field of COMPASS is applied to simulations in order to compute interfacial and solubility parameters. Molecular dynamics approach to investigate the interaction and adsorption manner of PCL with metal oxides. Whereas investigations are useful in exploring polymer composites. Much better adhesion is achieved by the calculations between the PCL oligomer and the metal oxides under investigation. The negative values of interaction energy have to be forecasted despite the presence of acid-base or hydrogen-bonding interactions.

Keywords: *Polycaprolactone, Molecular dynamics, interaction energy, metal oxides.*

1. Introduction

Mixtures of metallic particles and polymers have many uses, e.g., in sensing, catalytic and medical applications[1], as well as manufacturing methods[2]. The metallic interface of polymers can vary effectively from its bulk manner. Whereas polymers have a surface excellence density, the action of the substances at the nano drastically results in the characteristics of the system at the macro[3]. Computational methods, such as Monte Carlo(MC)[4], molecular dynamics(MD)[5], and dissipative particle dynamics(DPD)[6], have engrossed much attention in this field. MD simulations have been applied by Fernandes et al.[7] and Negreiros et al.[8] to investigate the interaction between water with iron and iron oxide surfaces, respectively. Using MD simulations, some other materials, including iron surfaces in ionic liquids[9], together with solid-liquid metals[10] have been investiagated.

MD and MC simulations have been applied by Mansfield and Theodorou[11] to investigate the adhesion and interaction of atactic polypropylene with graphite. Matsuda et al.[12] investigated n-alkane melt's MD simulations at temperatures of 300 K and 400 K in attractive generic and neutral, as well as crystalline surfaces. Gooneie et al.[13] offered a modeling method to simulate the interface among a narrow film of polyethylene melt based on a semi-infinite graphite stratum. Kacar et al.[14] presented surface MD models that were large-grained into DPD models. MD simulations have been performed to investigate the interaction of poly (n-butyl acrylate-co-acrylic acid) and (n-butyl acrylate) with α-quartz, α-ferrite, and α-ferric oxide by Anastassiou and Mavrantzas[15]. Liu et al.[16], using the MD method, showed that the surface of CdS_2 improved in the exposure of mercapto propyl tri methoxy silane. Ta et al.[17] carried out MD simulations to study the adsorption energies and structural properties of alkanes on iron and its oxide surfaces.

Polycaprolactone(PCL) is biocompatible, biodegradable, biocompatible, and also easy to process from aqueous solutions. It may be applied in implants[18], controlled drug delivery systems[19], scaffolds in tissue engineering[20], food packaging[21], medical devices, and bio packaging[22]. Also, it is a semicrystalline polymer that has previously been largely utilized in several applications. Recently, metal oxides, such as TiO_2[23], ZrO_2[24], ZnO[25], Al_2O_3[26], and SiO_2[27], have been used for the combination with the polymer. PCL-based metal oxides, including biomaterials to use in tissue engineering and drug release, have been increasingly under focus due to the biocompatibility or cytotoxicity with tuned biodegradation and mechanical strength. Several types of PCL- metal oxides besides its copolymers have been recorded[28]. Using the solution casting method, Mallakpour and Nouruzi[29] have synthesized PCL/ZnO NCs. Melt mixing method has been employed by Mofokeng and Luyt[30] to provide PLA/ PCL blend NCs with TiO_2 as the filler. Also, Wang et al.[31] employed PCL/Fe_3O_4 NCs in an in situ polymerization technique. PCL/ZnO membranes have been fabricated by Augustine et al.[32] in 2016. In this study, PCL is selected as a model polymer to investigate its interactions with metal oxides, such as ZnO, CuO, hematite (Fe_2O_3), NiO and silica (SiO_2) applying MD simulation method.

*e-mail: nmmadady@gmail.com

2. Modeling Details

Molecular simulations are carried out by Material Studio (6.0) software[33]. The simulation approach consists of molecular dynamics and mechanics calculations utilizing the Forcite module[34]. The force field of COMPASS (condensed-phase optimized molecular potentials for atomistic simulation studies) is used for MD simulation, being one of the first ab initio force field methods validated and parameterized by the condensed-phase features[35]. In all the simulations, the temperature is equilibrated with the Andersen algorithm[36]. The velocity Verlet algorithm[37] was then applied to integrate the equations of motion. The non-bonded interactions have been calculated using group-based method with vidid atom sums being calculated to 9.5 A˚ . The tail correction was used to non-bonded interactions during the MD run.

The oligomer chain of polycaprolactone is made with 10 monomer units with $C_{66}H_{112}O_{22}$ formula.

Polycaprolactone is optimized, and its energy is minimized. According to the relative densities of the selected oligomers, amorphous cells are generated. The method used in constructing the amorphous cell module of MS modeling was the combined use of an algorithm expanded by Theodorou and Suter[38] and the scanning method of Meirovitch[39].

Generated amorphous cells are optimized to a convergence level of 0.01 kcal/mol/A° employing the former technique. Applying the Forcite modules, constant volume and temperature ensemble are chosen for MD simulations. The optimized structures with 3D grating are steadied in the NVT ensemble at 298 K. MD run for 100 ps are carried out for eliminating the unsuitable local minima.

This make sures that a relatively thin layer would feel the effective pressure equivalent to that in the bulk. Because the system includes a vacuum space, both the PCL and metal oxids systems are free to expand even though the ensemble is at a constant volume. The unit cell structure of metal oxides comes to exist with the Material studio Software. Whereof they are crystal structures provided experimentally, the lattice parameters are the experimental ones. Symmetry, space group, and lattice parameters of studied metal oxides are given in Table 1. The most stable surface of Hematite (001), SiO2 (100), CuO(101), NiO(111) and ZnO wurtzite structure (001) were used as a surface against which PCL was brought in contact during the simulation step.

As regards the bonds between oxygen atoms and metal being ionic, in essence, the parameters do not form covalent bonds among them; therefore, the bonds have to be put away in optimization and minimization. Using the surface builder module of MS modeling, metal oxide surfaces are prepared by the preferred cleave planes that provide the surface fractional depth to be more than the non-bonded cut-off distance of 9.5 A°.The build vacuum slab crystal is applied for building a crystal from a surface. The crystal is constructed by repeating the surface in a given direction using a repeat distance which is greater than the surface thickness. This introduces a region of vacuum between the surface units. The crystal surface of the metal oxide slab, which is used in the simulation box to examine the adhesion calculation, is designed in MS modeling by the crystal builder facility.

The PCL is assembled in the simulation box with the metal oxide surface, and c-dimension of the box is extended to 30A°. Then, the MD simulation is performed 30,000 steps with a time step of 1 fs at 298 K. Surface atoms all are inhibited in NVT dynamics as, in the earlier step, the metal oxide surface is minimized. Figure 1 illustrates the final structures the PCL simulated structure with metal oxides after MD simulations. The interaction energy or adhesion energy is computed based on Equation (1). Firstly, the energy (E_{total}) for the simulation box with both PCL and surface atoms is computed, and then without the surface, the PCL energy (E_{PCL}) is calculated. Eventually, the surface atoms are retained, and PCL is removed to calculate the surface energy ($E_{surface}$). Next, the interaction energy or adhesion energy of PCL and the surface is computed as:

$$E_{interaction} = \frac{E_{total} - \left(E_{surface} + E_{PCL}\right)}{V} \quad (1)$$

where V is the molar volume of PCL.

3. Results and Discussion

The calculation of the interaction energy of metal oxides is vital to realize the metal oxides' physisorption with PCL. The metal oxide surface modeling is the core phase in computing interaction energy[40]. In the present work, the quartz crystalline structure of SiO_2, ZnO, and $Fe_2O_3$with a hexagonal symmetry, CuO with Monoclinic, as well as NiO with Cubic symmetry, are considered. In the main step, adhesion raises with a decline in the energy of the surface. It should be pointed out that a direct concordance exists between the ideas of 'surface energy' and 'surface stability,' that is to say surfaces with lower surface energy are more stable and vice versa.

C=O and C-O groups are the leading sites of interaction with metal oxide surfaces in PCL. It is assumed that the C-O-C bond's intensity ratio drops compared with the C=O one. The outcome energy and orientation of PCL adsorbed on five diverse metal oxide surfaces are compared.

Table 1. Symmetry, space group and lattice parameters of studied metal oxides

Metal-oxides	Space Group	Symmetry	Lattice parameters	
			Lenths(A^0)	Angles(degrees)
NiO	FM-3M	Cubic	a=b=c=4.17	α=β=9, γ=120
$SiO_{2\ quartz}$	P3121	Hexagonal	a=b=4.91,c= 5.40	α=β=90, γ=120
CuO	C2/C	Monoclinic	a= 4.65, b= 3.41, c= 5.108	α= γ=90, β=100
ZnO	P63MC	Hexagonal	a=b= 3.24, c= 5.20	α=β=90, γ=120
Fe_2O_3	R-3C	Hexagonal	a=b=5.03, c=13.72	α=β=90, γ=120

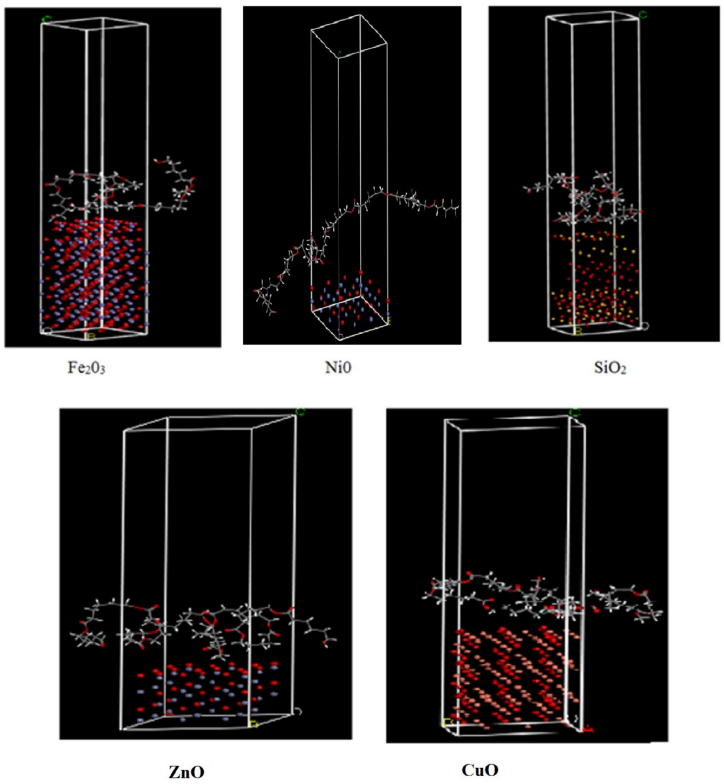

Figure 1. PCL simulated structure with metal oxides(optimized).

A similar configuration is observed for PCL with other metal oxide surfaces, but not presented to withhold plenty here. In the case of Fe_2O_3, the energy needed for distinct segments of PCL from hematite (namely, the adhesive energy value) is calculated as -128.90kcal/mol. For NiO, similarly, the energy is found to be -41.67 kcal/mol. Also, for SiO2, CuO, and ZnO, the computed adhesive energies are -86.55, -111.93, and -10.88 kcal/mol, respectively. It is specified that in the metal oxide of Fe_2O_3, the interaction energy is remarkably greater than other metal oxides; however, CuO and silica display excellent adhesiveness that is definite from its adhesion energy value. The NiO interaction energy value is modest than those of other metal oxide surfaces, showing their lesser adherence to PCL. Also, the interaction energy value of ZnO is the lowest. The energy of the surface, polymer, as well as total and interaction energies of metal oxides with the PCL surface model are provided in Table 2.

Also , theoretical simulations of such interactions were calculated through vibrational modes. In this portion, have been computed the vibrational modes of PCL with chosen metal oxides via instantaneous normal mode analysis[41]. The vibrational modes were obtained by employing the CASTEP module. As the force constants are well defined, the vibrational absorptions can be calculated with a capable accuracy and have been examined the interaction between metal oxide and the C=O group of PCL from the intensities of vibrational modes. In PCL, the primary site of interaction with metal oxide surface is C=O and C-O groups[42]. From the spectroscopic data of PCL, vibrational modes of C=O is measured to be in the range of 1715-1730 cm^{-1} and C-O-C is measured to be in the range of 1163-1210 cm^{-1}.

Table 2. Vibrational frequencies and interaction energies for the chosen metal oxides and PCL interfaces

Metal-oxides	Frequency of C=O (cm^{-1})	E_{int} (kcal/mol)
NiO_2	1690	-41.67
$SiO_{2\ quartz}$	1685	-86.55
CuO	1710	-111.93
ZnO	1612	-10.87
Fe_2O_3	1719	-128.90

The simulated frequencies for PCL/metal interfaces are given in Table 2, trend of the Frequency of C=O bond as compared to C=O bond of PCI. Thus, it is clear that the Frequency of C=O bond becomes less upon interaction with metal oxides; it also follows that Frequency of C=O bond weakens upon interaction with metal oxides increases in an order for metal oxides having less preference for interaction with PCL. Therefore, the calculation of adhesive character of the studied metal oxides with PCL through the intensity ratio of C=O bond by the vibrational modes assign credible approximations with the obtained interaction energies.

Charge density difference can be investigated taking the superposition of non-interacting atoms as reference and allows us to analyze atomic bonds but misses global redistributions of charge. This presedure makes it possible to realize global effects of interaction in surface redistribution due to the presence of the other set. Materials Studio provides the option of generating the electron density difference with respect to a linear combination of the densities of sets of atoms included

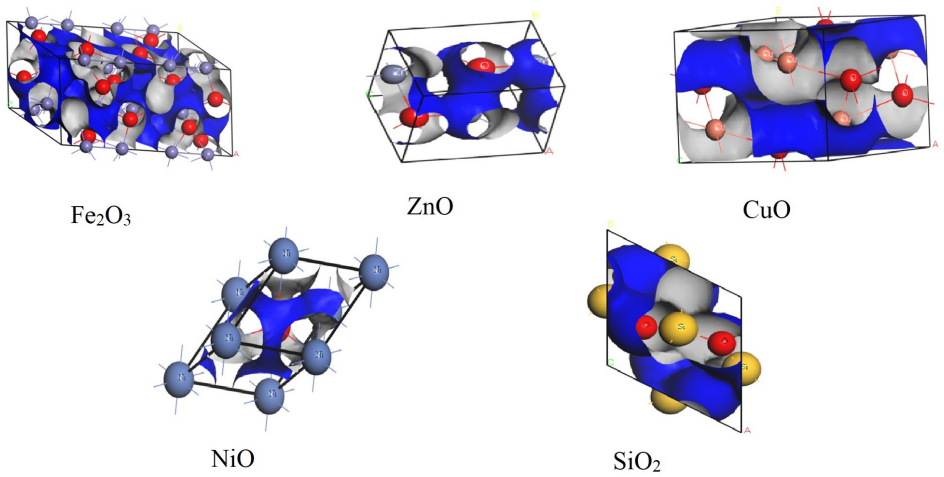

Figure 2. Charge density plots of metal oxides(unit cell).

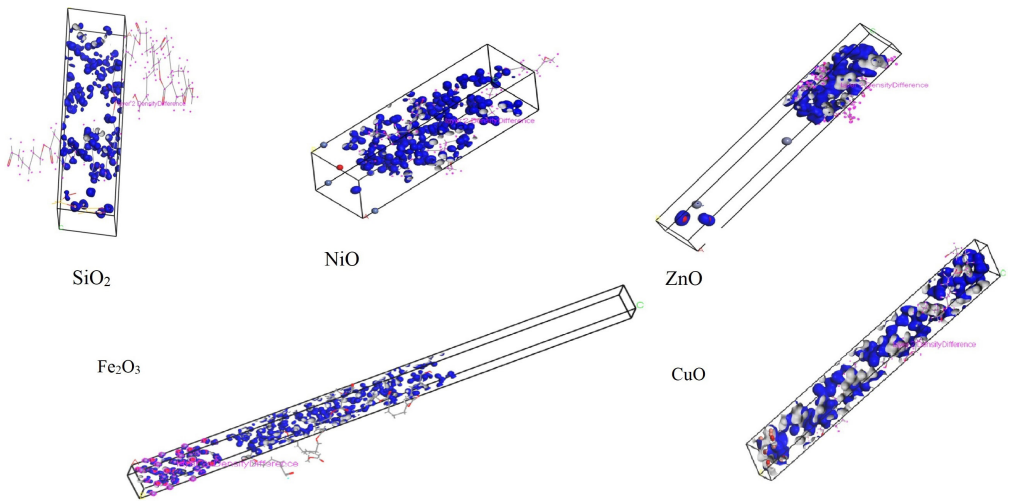

Figure 3. Charge density differnce plots of metal oxides(unit cell)/PCL interface.

in the model. Which generates a density difference field which effectively corresponds only to the formation of bonds between atoms in different sets and to charge redistribution within the sets that is due to the presence of other sets. This property is impotant to explain such processes as bonding of molecules to internal and external surfaces, or modeling of large molecules from smaller fragments. Ground state charge densities were investigated using CASTEP modules. Exchange and correlation interactions were treated through the generalized gradient approximation in the interpretation GGA-PBE[43]. The atomic charges of atoms in Fe_2O_3 crystals were set to 1.2 and −0.8 for Fe and O atoms, respectively. Also, the atomic charges of atoms in CuO and NiO crystals were set to 0.8 and −0.8 for Ni, Cu and O atoms. Charge density difference of pure metal oxides and intraction with PCLin Figure 2 and Figure 3 have been illustrated. In this plot a loss of electrons is indicated in blue, while electron enrichment is indicated in red. White indicates regions with very little change in the electron density. The charge density near the vacuum surface is very important to the vacuum potential energy. The plots of total charge density and charge density difference are illustrated as an isosurface in Figure 2 and Figure 3. These plots confirm that the interaction between PCL and metal oxides are driven by electrostatics. Chiefly , the charge density difference plot clearly shows that there is redistribution of electrons between PCL and metal oxides. PCL polymer and metal oxides have acidic or basic sites which can interact to increase adsorption, charge-transfer, wettability and adhesion. These polar interactions are independent of dipole moments and occur only when one material has acid groups which can interact with basic groups of the other material.

4. Conclusion

This study provides a good insight into polymer-non-polymer interfacial interactions by molecular modeling procurement. The negative values of interaction energy have to be forecasted despite the presence of strong acid-base or hydrogen-bonding interactions. Enhancement negative values of interaction energies excuse mutual solubility of the polymer pair increase. Although the interfacial study

of PCL and metal oxides considers the designation of PCL adhesion with five metal oxides (Fe_2O_3, CuO, NiO, SiO_2, and ZnO), the calculations display a better adhesion among PCL oligomer and the metal oxides under investigation. The interfacial chemistry assessment among polymers and different metal oxides makes a base able to synthesize and sketch nanoclusters.

5. Acknowledgements

I gratefully thank Payame Noor University for financial support. The author would like to express their appreciations to department of chemistry this university for providing research facilities.

6. References

1. Minnai C, Milani P. Metal-polymer nanocomposite with stable plasmonic tuning under cyclic strain conditions. Appl Phys Lett. 2015;107(7):073106-31.
2. Gwon TM, Kim JH, Choi GJ, Kim SJ. Mechanical interlocking to improve metal–polymer adhesion in polymer-based neural electrodes and its impact on device reliability. J Mater Sci. 2016;51(14):6897-912.
3. Johnston K, Harmandaris V. Hierarchical simulations of hybrid polymer-solid materials. Soft Matter. 2013;9(29):6696-710.
4. Daoulas K, Harmandaris VA, Mavrantzas VG. Detailed atomistic simulation of a polymer melt/solid interface: Structure, density, and conformation of a thin film of polyethylene melt adsorbed on graphite. Macromolecules. 2005;38(13):5780-95.
5. Rissanou A, Power A, Harmandaris V. Structural and dynamical properties of polyethylene/graphene nanocomposites through molecular dynamics simulations. Polymers. 2015;7(3):390-417.
6. Gooneie A, Schuschnigg S, Holzer C. Orientation of anisometric layered silicate particles in uncompatibilized and compatibilized polymer melts under shear flow. Macromol Theory Simul. 2016;25(1):85-98.
7. Fernandes FW, Campos T, Cividanes LS, Simonetti E, Thim GP. Adsorbed water on iron surface by molecular dynamics. Appl Surf Sci. 2016;362:70-8.
8. Negreiros FR, Pedroza LS, Dalpian GM. Effect ofchargeson theinteraction ofa watermolecule withthe Fe2O3(0001) surface. J Phys Chem C. 2016;120(22):11918-25.
9. Mendonca A, Malfreyt P, Padua A. Interactions and ordering of ionic liquids at a metal surface. J Chem Theory Comput. 2012;8(9):3348-55.
10. Bernardes C, Canongia Lopes JN, Piedade MEM. All-atom force field form olecular dynamics simulations on organo transition metal solid sand liquids. Application to M(CO) n(M=Cr,Fe,Ni,Mo,Ru,orW) compounds. J Phys Chem A. 2013;117(43):11107-13.
11. Mansfield KF, Theodorou D. Molecular dynamics simulation of a glassy polymer surface. Macromolecules. 1991;24(23):6283-94.
12. Matsuda T, Smith GD, Winkler RG, Yoon DY. Stochastic dynamics simulations of n-alkane melts confined between solid surfaces: influence of surface properties and comparison with scheutjens-fleer theory. Macromolecules. 1995;28(1):165-73.
13. Gooneie A, Schuschnigg S, Holzer C. Orientation of anisometric layered silicate particles in uncompatibilized and compatibilized polymer melts under shear flow. Macromol Theory Simul. 2016;25(1):85-98.
14. Kacar G, Peters E, De With G. Structure of a thermoset polymer near an alumina substrate as studied by dissipative particle dynamics. J Phys Chem C. 2013;117(37):19038-47.
15. Anastassiou A, Mavrantzas VG. Molecular structure and work of adhesion of poly(n-butyl acrylate) and poly(n-butyl acrylate-co-acrylic acid) on -quartz,-ferric oxide, and -ferrite from detailed molecular dynamics simulations. Macromolecules. 2015;48(22):8262-84.
16. Liu H, Espe M, Modarelli DA, Arias E, Moggio I, Ziolo RF, et al. Interaction of substituted poly(phenyleneethynylene)s with ligand-stabilized CdS nanoparticles. J Mater Chem A Mater Energy Sustain. 2014;2(23):8705-11.
17. Ta TD, Tieu AK, Zhu H, Kosasih B. Adsorption of normal-alkanes on Fe(110), FeO(110), and Fe2O3(0001): influence of iron oxide surfaces. J Phys Chem C. 2015;119(23):12999-3010.
18. Kashanian S, Harding F, Irani Y, Klebe S, Marshall K, Loni A, et al. Evaluation of mesoporous silicon/ polycaprolactone composites as ophthalmic implants. Acta Biomater. 2010;6(9):3566-72.
19. Schlesinger E, Ciaccio N, Desai TA. Polycaprolactone thin-film drug delivery systems: empirical and predictive models for device design. Mater Sci Eng C. 2015;57:232-9.
20. Yeong WY, Sudarmadji N, Yu HY, Chua CK, Leong KF, Venkatraman SS, et al. Porous polycaprolactone scaffold for cardiac tissue engineering fabricated by selective laser sintering. Acta Biomater. 2010;6(6):2028-34.
21. Elen K, Murariu M, Peeters R, Dubois P, Mullens J, Hardy A, et al. Towards high-performance biopackaging: barrier and mechanical properties of dual-action polycaprolactone/zinc oxide nanocomposites. Polym Adv Technol. 2012;23(10):1422-8.
22. Mondal D, Griffith M, Venkatraman SS. Polycaprolactone-based biomaterials for tissue engineering and drug delivery: current scenario and challenges. Int J Polym Mater. 2016;65(5):255-65.
23. Mallakpour S, Jarang N. Exploration of the role of modified titania nanoparticles with citric acid and vitamin C in improvement of thermal stability, optical property, and mechanical behavior of novel poly(vinyl chloride) nanocomposite films. Journal of Vinyl and Additive Technology. 2017;23:E15-24.
24. Mallakpour S, Nezamzadeh A. Polymer nanocomposites based on modified ZrO2 NPs and poly(vinyl alcohol)/poly(vinyl pyrrolidone) blend: optical, morphological and thermal properties. journal. Polym Plast Technol Eng. 2016;56(10):1136-45.
25. Mallakpour S, Javadpour M. The potential use of recycled PET bottle in nanocomposites manufacturing with modified ZnO nanoparticles capped with citric acid: preparation, thermal, and morphological characterization. RSC Advances. 2016;6(18):15039-47.
26. Mallakpour S, Dinari M. Enhancement in thermal properties of poly(vinyl alcohol) nanocomposites reinforced with Al2O3 nanoparticles. J Reinf Plast Compos. 2013;32(4):217-24.
27. Mallakpour S, Khani Z. Use of vitamin B1 for the surface treatment of silica (SiO2) and synthesis of poly(vinyl chloride)/ SiO2 nanocomposites with advanced properties. Polym Bull. 2017;74(9):3579-94.
28. Singh NK, Maiti P. Polycaprolactone based nanobiomaterials. Hoboken: John Wiley & Sons; 2012.
29. Mallakpour S, Nouruzi N. Effect of modified ZnO nanoparticles with biosafe molecule on the morphology and physiochemical properties of novel polycaprolactone nanocomposites. Polymer. 2016;89:94-101.
30. Mofokeng J, Luyt A. Morphology and thermal degradation studies of melt-mixed poly (lactic acid)(PLA)/poly (ε-caprolactone) (PCL) biodegradable polymer blend nanocomposites with TiO2 as filler. Polym Test. 2015;45:93-100.
31. Wang G, Wang L, Wei Z, Sang L, Dong X, Qi M, et al. Synthesis and characterization of poly (ε-caprolactone)/Fe3O4 nanocomposites by in situ polymerization. Chin J Polym Sci. 2013;31(7):1011-21.
32. Augustine R, Kalarikkal N, Thomas S. Effect of zinc oxide nanoparticles on the in vitro degradation of electrospun polycaprolactone membranes in simulated body fluid. Int J Polym Mater Polym Biomater. 2016;65(1):28-37.
33. Accelrys Inc. MS modeling. San Diego: Accelrys Inc.; 2008.

34. Lippa KA, Sander LC, Mountain RD. Molecular dynamics simulations of alkylsilane stationary-phase order and disorder. 2. Effects of temperature and chain length. Anal Chem. 2005;77(24):7852-61.
35. Sun H. COMPASS: An ab Initio Force-Field Optimized for Condensed –phase application. J Phys Chem B. 1998;102(38):7338-64.
36. Andersen HC. Molecular dynamics simulations at constant pressure and/or temperature. J Chem Phys. 1980;72(4):2384-9.
37. Verlet L. Computer "experiments" on classical fluids. I. thermodynamical properties of Lennard-Jones molecules. Phys Rev. 1967;159(1):98-104.
38. Theodorou DN, Suter UW. Detailed molecular structure of a vinyl polymer glass. Macromolecules. 1985;18(7):1467-78.
39. Meirovitch HJ. Computer simulation of self-avoiding walks: testing the scanning method. J Chem Phys. 1983;79(1):502-9.
40. Cooper TG, Leeuw NH. A computer modeling study of the competitive adsorption. Langmuir. 2004;20(10):3984-94.
41. Nonella M, Mathias G, Tavan P. Infrared spectrum of *p*-benzoquinone in water obtained from a QM/MM hybrid molecular dynamics Simulation. J Phys Chem A. 2003;107(41):8638-47.
42. Kemala T, Budianto E, Soegiyono B. Preparation and characterization of microspheres based on blend of poly(lactic acid) and poly(e-caprolactone) with poly(vinyl alcohol) as emulsifier. Arab J Chem. 2012;5(1):103-8.
43. Perdew JP, Burke K, Wang Y. Generalized gradient approximation for the exchange-correlation hole of a many-electron system. Phys Rev B Condens Matter. 1996;54(23):16533-9.